

# HER3 Augmentation via Blockade of EGFR/AKT Signaling Enhances Anticancer Activity of HER3-Targeting Patritumab Deruxtecan in EGFR-Mutated Non-Small Cell Lung Cancer



Kimio Yonesaka<sup>1</sup>, Junko Tanizaki<sup>1,2</sup>, Osamu Maenishi<sup>3</sup>, Koji Haratani<sup>1</sup>, Hisato Kawakami<sup>1</sup>, Kaoru Tanaka<sup>1</sup>, Hidetoshi Hayashi<sup>1</sup>, Kazuko Sakai<sup>4</sup>, Yasutaka Chiba<sup>5</sup>, Asuka Tsuya<sup>6</sup>, Hiroki Goto<sup>7</sup>, Eri Otsuka<sup>7</sup>, Hiroaki Okida<sup>7</sup>, Maki Kobayashi<sup>7</sup>, Ryoto Yoshimoto<sup>7</sup>, Masanori Funabashi<sup>7</sup>, Yuuri Hashimoto<sup>8</sup>, Kenji Hirotani<sup>9</sup>, Takashi Kagari<sup>8</sup>, Kazuto Nishio<sup>4</sup>, and Kazuhiko Nakagawa<sup>1</sup>

## ABSTRACT

**Purpose:** EGFR-tyrosine kinase inhibitor (TKI) is a standard first-line therapy for activated *EGFR*-mutated non-small cell lung cancer (NSCLC). Treatment options for patients with acquired EGFR-TKI resistance are limited. HER3 mediates EGFR-TKI resistance. Clinical trials of the HER3-targeting antibody–drug conjugate patritumab deruxtecan (HER3-DXd) demonstrated its anticancer activity in *EGFR*-mutated NSCLC; however, the mechanisms that regulate HER3 expression are unknown. This study was conducted with the aim to clarify the mechanisms underlying HER3 regulation in *EGFR*-mutated NSCLC tumors and explored the strategy for enhancing the anticancer activity of HER3-DXd in *EGFR*-mutated NSCLC.

**Experimental Design:** Paired tumor samples were obtained from 48 patients with *EGFR*-mutated NSCLC treated with EGFR-TKI(s). HER3 expression was immunohistochemically quantified with H-score, and genomic alteration and transcriptomic signature were

tested in tumors from pretreatment to post-EGFR-TKI resistance acquisition. The anticancer efficacy of HER3-DXd and osimertinib was evaluated in *EGFR*-mutated NSCLC cells.

**Results:** We showed augmented HER3 expression in *EGFR*-mutated tumors with acquired EGFR-TKI resistance compared with paired pretreatment samples. RNA sequencing revealed that repressed PI3K/AKT/mTOR signaling was associated with HER3 augmentation, especially in tumors from patients who received continuous EGFR-TKI therapy. An *in vitro* study also showed that EGFR-TKI increased HER3 expression, repressed AKT phosphorylation in multiple *EGFR*-mutated cancers, and enhanced the anticancer activity of HER3-DXd.

**Conclusions:** Our findings help clarify the mechanisms of HER3 regulation in *EGFR*-mutated NSCLC tumors and highlight a rationale for combination therapy with HER3-DXd and EGFR-TKI in *EGFR*-mutated NSCLC.

## Introduction

EGFR-tyrosine kinase inhibitor (TKI) constitutes a standard first-line therapy for patients with non-small cell lung cancer (NSCLC) harboring an EGFR-activating mutation (1–3). EGFR-TKI induces

substantial tumor regression in patients with *EGFR*-mutated NSCLC; however, all tumors eventually acquire resistance to EGFR-TKIs (4). Among the various mechanisms underlying EGFR-TKI resistance, *EGFR* secondary mutations, including T790M missense mutation, induce resistance in approximately 50% of first- and second-generation EGFR-TKIs; C797S mutation accounts for approximately 15% of the resistance to the third-generation EGFR-TKI osimertinib (5–7). These mutations cause an amino acid substitution that prevents EGFR-TKI from binding to the EGFR-kinase domain (5, 7). Alternatively, the aberrant MET-mediated or HER2 activation-mediated bypassing-cell signaling causes EGFR-TKI resistance in *MET*- or *HER2*-amplified NSCLCs (8, 9). Multiple strategies to conquer the limitations of EGFR-TKI therapy are in different clinical development stages (4, 10). Next-generation EGFR-TKIs may overcome secondary EGFR mutation-mediated resistance, whereas MET inhibitors may counter MET alteration-mediated resistance (11–13). In a limited subpopulation, MET amplification occurred in 10%–20% of patients with EGFR-TKI resistance, and they can benefit from MET inhibitor therapy, whereas the remaining 80%–90% of patients will require further evidence-based treatment optimization (11–13).

HER3 is a member of the HER family and aberrant HER3 expression is associated with poor prognosis in various cancers, including NSCLC (14, 15). HER3, with its impaired kinase activity, cannot be autophosphorylated, but can be transphosphorylated by coupling with other receptor tyrosine kinases (RTK; e.g., EGFR, HER2, or MET; ref. 16). Activated HER3 provides multiple docking

<sup>1</sup>Department of Medical Oncology, Kindai University Faculty of Medicine, Osaka-sayama, Osaka, Japan. <sup>2</sup>Department of Medical Oncology, Kishiwada City Hospital, Kishiwada, Osaka, Japan. <sup>3</sup>Department of Pathology, Kindai University Faculty of Medicine, Osaka-sayama, Osaka, Japan. <sup>4</sup>Department of Genome Biology, Kindai University Faculty of Medicine, Osaka-sayama, Osaka, Japan. <sup>5</sup>Clinical Research Center, Kindai University Hospital, Osaka-sayama, Osaka, Japan. <sup>6</sup>Department of Medical Oncology, Izumi City General Hospital, Izumi, Osaka, Japan. <sup>7</sup>Translational Research Department, Daiichi Sankyo RD Novare Co., Ltd., Edogawa, Tokyo, Japan. <sup>8</sup>Oncology Research Laboratories I, Research Function, R&D Division, Daiichi Sankyo Co., Ltd., Shinagawa, Tokyo, Japan. <sup>9</sup>Early Clinical Development Department, Development Function, R&D Division, Daiichi Sankyo Co., Ltd., Shinagawa, Tokyo, Japan.

**Note:** Supplementary data for this article are available at Clinical Cancer Research Online (<http://clincancerres.aacrjournals.org/>).

**Corresponding Author:** Kimio Yonesaka, Department of Medical Oncology, Kindai University Faculty of Medicine, 377-2 Ohno-higashi, Osaka-Sayama-shi, Osaka 589-8511, Japan. Phone: 817-2366-0221; Fax: 817-2360-5000; E-mail: yonesaka@med.kindai.ac.jp

Clin Cancer Res 2022;28:390–403

doi: 10.1158/1078-0432.CCR-21-3359

©2021 American Association for Cancer Research

### Translational Relevance

EGFR-tyrosine kinase inhibitor (TKI) is a standard therapy for activated *EGFR*-mutated non-small cell lung cancer (NSCLC). However, treatment options are limited for tumors acquiring a resistance to EGFR-TKIs. In this study, we showed augmented HER3 expression in *EGFR*-mutated tumors with acquired EGFR-TKI resistance compared with paired pretreatment samples. Repressed PI3K/AKT/mTOR signaling was associated with HER3 augmentation, especially in tumors from patients who received continuous EGFR-TKI therapy beyond tumor progression. An *in vitro* study showed that EGFR-TKI increased HER3 expression in multiple *EGFR*-mutated cancers, and enhanced the anticancer activity of the HER3-targeting antibody–drug conjugates patritumab deruxtecan (HER3-DXd). Our findings highlight a rationale for combination therapy with HER3-DXd and EGFR-TKI in *EGFR*-mutated NSCLC that is currently being evaluated in a clinical trial for patients with *EGFR*-mutated NSCLC tumors, not only with regard to an acquired resistance to EGFR-TKI but also in EGFR-TKI-naïve tumors (NCT04676477).

sites for PI3K and amplifies signaling in the PI3K/AKT/mTOR pathway for cell survival (17). HER3 plays an essential role in EGFR-TKI resistance in *EGFR*-mutated NSCLC; for example, aberrant METs due to *MET* amplification when coupled with HER3s can lead to PI3K/AKT/mTOR signaling in tumors during EGFR-TKI therapy (8). Moreover, the HER3 ligand heregulin induces HER2/HER3 coupling and signaling for cancer cell survival independently from the EGFR (18). Therefore, HER3 is considered to be one of the targets for anticancer treatment, especially in *EGFR*-mutated NSCLC (14, 16).

Currently, antibody–drug conjugates (ADC) have demonstrated significant anticancer activity against cancers that are refractory to anticancer treatment (19–21). ADC, on binding to the cell-surface antigen, is internalized into the cytoplasm and subsequently releases its payload to damage DNA or induce other effects (19). The HER3-targeting ADC patritumab deruxtecan (HER3-DXd) demonstrated anticancer activity based on HER3 expression for several cancer types, including *EGFR*-mutated NSCLC (22–24). In a phase I clinical trial, HER3-DXd demonstrated durable tumor regression in patients with *EGFR*-mutated NSCLCs despite heavy pretreatment with EGFR-TKIs and chemotherapy (25). Although the HER3 expression level tended to correlate with HER3-DXd efficacy in the trial, there is limited evidence of HER3 expression being influenced by EGFR inhibition and the underlying mechanism that regulates HER3 expression in *EGFR*-mutated tumors (26).

This study was conducted with the aim to clarify the mechanisms underlying HER3 regulation in *EGFR*-mutated NSCLC tumors through genomic and transcriptome analysis using 48 paired tissue samples that were obtained from patients with *EGFR*-mutated NSCLC who acquired resistance to EGFR-TKI.

## Materials and Methods

### Study design

This retrospective study involved HER3 protein expression, a genomic and transcriptome analysis of 48 paired tissue samples that were obtained from patients with *EGFR*-mutated NSCLC with acquired resistance to EGFR-TKI.

### Tumor samples and clinical data

Specimens were obtained from archived formalin-fixed paraffin-embedded (FFPE) histological sections of 48 paired tumors from 48 patients with *EGFR*-mutated NSCLC who were treated at the Kindai Hospital, Kishiwada Hospital, and Izumi Hospital (Osaka, Japan) between 2018 and 2020. Most of the tumor samples were obtained from the lung via a bronchoscopic diagnostic biopsy or surgical resection. The samples before EGFR-TKI treatment were paired to samples obtained at the time when acquired resistance to EGFR-TKI was detected. Clinical data were collected from the medical records of each patient. This study is conducted in accordance with the Declaration of Helsinki, and was approved by the respective Institutional Review Boards of Kindai Hospital, Kishiwada Hospital, and Izumi Hospital (Osaka, Japan). Written informed consent was obtained from all participants after an opportunity for optout from this study was provided.

### IHC staining

HER3 expression in the membranous tumor was evaluated by IHC in *EGFR*-mutated NSCLC tumoral tissues using previously reported methods (26). Sections (thickness, 4  $\mu$ m) were immunologically stained for HER3 with an anti-HER3 mouse mAb (Cell Signaling Technology, Inc.; diluted 1.0  $\mu$ g/mL) using an automated slide stainer, DAKO Link48 (Agilent Technologies, Inc.). The IHC expression of HER3 in the membranes of cancer cells was interpreted by two pulmonary pathologists (O. Maenishi and E. Enoki) who were blinded to the study group allocation. The HER3 staining was scored on a continuous scale of 0–300, based on the percentage of cells with different staining intensities. Membrane staining was scored according to four categories: 0 for “no staining,” 1 + for “light staining visible only at high magnification,” 2 + for “intermediate staining,” and 3 + for “dark staining of linear membrane, visible even at low magnification.” The percentage of cells at different staining intensities was determined by visual assessment, and the score was calculated using the following formula:

$$\text{Score} = 1 \times (\% \text{ of } 1 + \text{ cells}) + 2 \times (\% \text{ of } 2 + \text{ cells}) + 3 \times (\% \text{ of } 3 + \text{ cells}).$$

### Cells and reagents

The *EGFR*-mutated NSCLC cell lines PC9, H1975, HCC4006, and HCC827 were obtained from the ATCC, and EGFR-TKI gefitinib-resistant HCC827GR5 cells from Dana-Farber Cancer Institute (Boston, MA). The authenticity of the cells was regularly tested by short tandem repeat. All of the above mentioned cell lines were characterized previously (8, 18). Cells were maintained in a humidified atmosphere of 5% CO<sub>2</sub> at 37°C in RPMI1640 medium (Sigma-Aldrich) supplemented with 10% FBS and 1% penicillin–streptomycin. Osimertinib, buparlisib, and ipatasertib were obtained from Selleck. Patritumab deruxtecan (HER3-DXd) was provided by Daiichi Sankyo Co., Ltd.

### DNA and RNA extraction

The FFPE specimens underwent histologic examination, and only specimens which contained sufficient tumor cells ( $\geq 50\%$  for RNA,  $\geq 30\%$  for DNA), as ascertained on hematoxylin and eosin staining, were subjected to nucleic acid extraction. DNA and RNA were purified using FormAPure (Beckman Coulter Inc.) or Allprep DNA/RNA FFPE kit (Qiagen) according to the manufacturer’s instructions. The quality and quantity of the DNA and RNA were verified using 4200 TapeStation (Agilent Technologies Inc.) and Qubit (Thermo Fisher Scientific Inc.), respectively. The extracted DNA/RNA was stored at  $-80^{\circ}\text{C}$  until the analysis.

Yonesaka et al.

### DNA panel sequencing

Library preparation was performed using Illumina TruSight Oncology 500 Kit (TSO500, Illumina Inc.) according to the manufacturer's instructions. We used a DNA input of 110 ng for library preparation; however, if the DNA amount was not sufficient, the maximum DNA input was used (details of the number of samples are shown in Supplementary Fig. S8). For optimal library preparation, the quality of DNA was assessed with Illumina FFPE QC Assay (Illumina, Inc.). We mixed 2 ng DNA with a QC Primer Reagent and 2 units of qPCR Master Mix (PowerUp SYBR Green Master Mix, Thermo Fisher Scientific Inc.), and qPCR was performed using the QuantStudio 12K Flex Real-Time PCR System (Thermo Fisher Scientific Inc.) according to the manufacturer's instructions. To fragment the DNA strands into 90–250 bp, the DNA of each sample was sheared using the Covaris E220 (Covaris, Inc.) using the following protocol: peak incident power, 75 W; duty factor, 15%; cycles per burst, 1,000; and treatment time, 180 seconds. The prepared libraries were quantified using the Qubit, and then normalized using Library Normalization Beads according to the manufacturer's instructions. The normalized libraries were sequenced using the NextSeq500 (Illumina, Inc.), 100 bp long from both ends ( $2 \times 100$  bp). The sequencing reads were aligned to human (hg19), and mutation call [single-nucleotide variant (SNV) and insertion/deletion] analysis was performed using the TSO500 analysis software (v1.3.1) and annotated using Variant Effect Predictor (VEP, release\_98.3). The tumor mutation burden (TMB) and copy-number variation analyses were also performed using the TSO500 analysis software versions 1.3.1 and 2.1, respectively. Samples with a low library concentration ( $<3$  ng/ $\mu$ L) were excluded, along with SNVs with low mutant allele count ( $<5$ ). Furthermore, known germline mutations in the Human Genetic Variation Database were excluded.

### RNA panel sequencing

Library preparation was performed using TSO500 according to the manufacturer's instructions. We used an RNA input of 170 ng for library preparation; however, if the RNA amount was not sufficient, the maximum RNA input was used (details of the number of samples are shown Supplementary Fig. S8). The prepared libraries were quantified using the Qubit and then normalized using the Library Normalization Beads according to the manufacturer's instructions. The normalized libraries were sequenced using the NextSeq500 or NextSeq550 (Illumina, Inc.), 100 bp long from both ends ( $2 \times 100$  bp). The sequencing reads were aligned to human (hg19). Fusion and splice variant calls were performed using TST170 analysis software (v2.0.0). Samples with a low library concentration ( $<3$  ng/ $\mu$ L) were excluded.

### Transcriptional profiling

RNA was extracted from FFPE tumors that contained  $>50\%$  cancer cells. The cDNA library for RNA sequencing (RNA-seq) was prepared for the directional sequencing method with the ribosomal RNA depletion and the unique-dual indexes using the following kits and reagents: QIAseq FastSelect (Qiagen Inc.), NEBNext Ultra II Directional RNA Library Prep Kit for Illumina (New England Biolabs, Inc.), and NEBNext Multiplex Oligos for Illumina (New England Biolabs, Inc.). We used an RNA input of 20 ng for library preparation; however, in case the RNA amount was not enough, the maximum RNA input was used (details of the number of samples are shown Supplementary Fig. S8). The quantity of the prepared library was evaluated by 4200 TapeStation. The prepared libraries were pooled in one tube and

sequenced on one flow cell at 1.5 nmol/L using the NovaSeq6000 (Illumina, Inc.), with 75 bp from both ends ( $2 \times 75$  bp). The sequencing reads were aligned with STAR software (2.5.3a) to human genome reference (GRCh38). The transcripts per million and expected count in each gene were estimated by RNA-seq using an expectation maximization (RSEM) software (1.3.0). Samples with non-cancer cells or low sum of expected counts were excluded and were normalized with the trimmed mean of M values normalization method. For the data analysis, samples with  $<50\%$  within a species or total reads of  $<50$ M were excluded.

### The Cancer Genome Atlas dataset

The Cancer Genome Atlas (TCGA) data on lung adenocarcinoma (LUAD) protein expression were used to evaluate HER3 and E-cadherin protein expression, which was measured by reverse phase protein array technology. These data have been normalized by the replicate-base normalization method. TCGA LUAD gene expression ascertained by RNA-seq was used to evaluate HER3, ZEB1/2, SNAI1/2, and TWIST1 mRNA expression, which were measured using IlluminaHiSeq\_RNASeqV2 and normalized by RSEM.

### Immunoblotting

Cells were seeded at a density of  $3 \times 10^6$  on 90-mm Prime Surface plates (Sumitomo Bakelite Co., Ltd.), incubated overnight in RPMI1640 medium containing 2% FBS, and harvested. Western blotting was performed as described previously. Proteins were probed using antibodies that were specific for phospho-EGFR (#2234, 1:1,000 dilution), phospho-AKT (#9271, 1:1,000 dilution), AKT (#9272, 1:1,000 dilution), cleaved PARP (#9541, 1:1,000 dilution), phospho-S6 (#4857, 1:1,000 dilution), S6 (#2217, 1:1,000 dilution), N-cadherin (#4061, 1:1,000 dilution), and vimentin (#3390, 1:1,000 dilution; all from Cell Signaling Technology); phospho-Histone H2A.X (#05-636, 1:2,000 dilution); Histone H2A.X (#11175, 1:10,000 dilution; Abcam); actin (#A5441, 1:7500 dilution; Sigma-Aldrich); and EGFR (#03, 1:200 dilution) and HER3 (#285, 1:1,000 dilution; Santa Cruz Biotechnology).

### Colony formation assay

HCC827 and HCC827GR5 cells were seeded at a density of  $3.0 \times 10^4$  per well in 6-well plates. After 24 hours, these cells were treated with 3  $\mu$ g/mL of HER3-DXd alone, 0.1  $\mu$ mol/L osimertinib alone, or both of these drugs in combination. The medium containing each drug was changed every 3 days. The cells were fixed with 10% buffered formalin phosphate for 5 minutes, and then stained with 0.2% crystal violet for 3 hours. After 14 days of incubation, the plates were gently washed with PBS and fixed with fixation solution (acetic acid/methanol 1:7) for 5 minutes. The plates were rinsed again with PBS and the colonies were stained with 0.5% crystal violet at room temperature for 2 hours. After staining, the plates were immersed in tap water to rinse off excess stain. The percentage colony area was automatically calculated using ImageJ 1.52a (NIH, Bethesda, MD) after image acquisition.

### siRNA transfection

siRNA against AKT was purchased (no. 443508; Nippon Gene). It consisted of 21-nucleotide sense and antisense strands. Non-targeting siRNA (siMock) was used as the nonspecific control. HCC827 cells were seeded at 50% confluence in 6-well plates, incubated for 24 hours in RPMI1640 medium supplemented with 0.5% FBS, and transfected with siRNAs using Lipofectamine RNAiMax (Invitrogen). After 48 hours, cells were harvested for Western blotting.

### Reverse transcription and real-time PCR

Total RNA was isolated from PC9 cells using the RNeasy Mini Kit (Qiagen) according to the manufacturer's instructions. cDNA was synthesized using the high-capacity RNA-to-cDNA kit (Applied Biosystems) and used in RT-PCR to quantitate HER3 expression. GAPDH was used as the internal control. Expression levels were determined using a standard method with an ABI 7900 HT system and SDS software (Applied Biosystems).

### Statistical analysis

Statistical analyses were performed using SPSS version 22.0 (IBM Corp.). Linear regression analysis was performed to investigate whether a factor, including EGFR-TKI administration, affected cell-surface HER3 expression. Pearson correlation coefficients ( $r$ ) were calculated to explore the relationships between HER3 expression level and other genomic expression in the tumors. Differences in genomic expression were compared by the mean differences. Graphical depictions of data were obtained using GraphPad Prism 5.0 for Windows (GraphPad Software, Inc.).

## Results

### HER3 expression in EGFR-mutated NSCLC tumors

In total, 48 paired samples were obtained before EGFR-TKI treatment and after the acquisition of EGFR-TKI resistance, designated as the "pretreatment sample" and "posttreatment sample," respectively, from patients with *EGFR*-mutated NSCLC whose tumors had initially responded to EGFR-TKI (Fig. 1A). Their cell-surface HER3 expression levels were immunohistochemically evaluated as the H-score (Fig. 1B and C); 81% of pretreatment samples (39/48) and 90% of posttreatment samples (43/48) expressed HER3 to various degrees (Fig. 1C). Cell-surface HER3 expression levels weakly correlated with HER3 mRNA levels in the pretreatment samples (Pearson  $r = 0.420$ ,  $n = 28$ ; Fig. 1D). Consistent with our observation, the HER3 protein expression level weakly correlated with the HER3 mRNA expression level in the lung adenocarcinoma cohort obtained from TCGA database (Pearson  $r = 0.438$ ,  $n = 360$ ; Fig. 1E) and the *EGFR*-mutant cohort (Pearson  $r = 0.635$ ,  $n = 26$ ; Supplementary Fig. S1; ref. 27).

Next, we explored the clinical or genomic backgrounds that correlated with cell-surface HER3 expression in the pretreatment samples. There was no significant relationship between the clinical characteristics, including smoking history, sex, and age, and the HER3 expression level (Fig. 1C; Pearson  $r = -0.014$ ,  $-0.165$ , and  $-0.002$ , respectively). According to the variances of *EGFR*, the type of EGFR-activating mutations did not correlate with the HER3 expression level (Fig. 1C; Pearson  $r = -0.009$ ), whereas the *EGFR* copy-number gain (CNG;  $\geq 4$  copies as the cut-off point) correlated with the HER3 level [mean value 115.8 and 53.5 for samples without *EGFR*-CNG ( $n = 37$ ) and those with *EGFR*-CNG ( $n = 10$ ), respectively ( $t$  test  $P = 0.042$ ; Fig. 1C and F)]. In agreement with our observation, the HER3 protein expression level was lower in *EGFR*-amplified tumors than in tumors with diploid *EGFR* in the lung adenocarcinoma cohort from TCGA database [difference between means (95% confidence interval) =  $-0.230$  ( $-0.435$  to  $-0.024$ ),  $t$  test,  $P = 0.029$ ; Fig. 1G] (27). The other concomitant variants, mutated *MYCN*, *RBI*, *p53*, and amplified *MYC* (frequencies: 7.1%, 9.5%, 50%, and 11.9%, respectively), showed no obvious relationship with HER3 expression in the pretreatment samples (Pearson  $r = 0.038$ ,  $-0.195$ ,  $0.047$ ,  $0.096$ ; Fig. 1C). The TMB had no obvious relationship with HER3 expression (Pearson  $r = 0.111$ ; Fig. 1C). In the posttreatment samples, the cell-surface HER3 expression was significantly increased as com-

pared with that in the pretreatment samples (mean value 100.8 vs. 155.9, paired  $t$  test  $P = 0.0007$ ; Fig. 1C and H). HER3 copy number was not different between pre samples and post samples (mean value 2.07 vs. 2.17, paired  $t$  test  $P = 0.3215$ ; Supplementary Fig. S2).

### Relationship between HER3 expression and epithelial-to-mesenchymal transition transcription factors

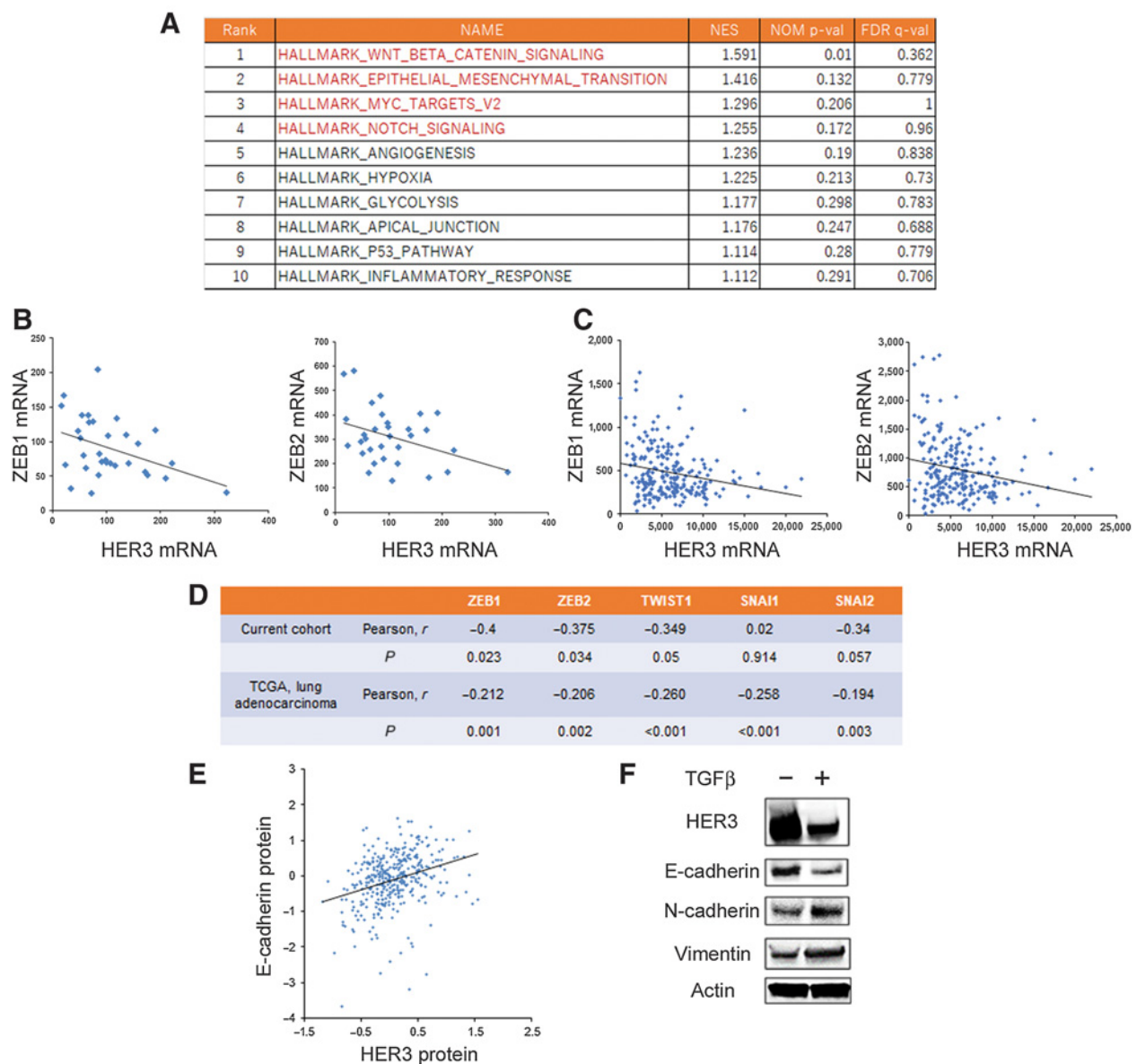
Gene set enrichment analysis (GSEA) was performed using pretreatment samples to screen for a relationship between the HER3 expression and the transcriptome profile of EGFR-TKI-naïve tumors (28). Thirty-two quantified samples were assigned to low and high cell-surface HER3 expression subgroups based on a median H-score of 70, and each subgroup was compared by the gene expression signature. The low HER3 expression group tended to have enriched genes that were related to the epithelial-to-mesenchymal transition (EMT), especially Wnt/ $\beta$ -catenin signaling, as compared with the high HER3 expression group (Fig. 2A). Therefore, we examined the relationship between the HER3 mRNA expression level and the expression level of the core EMT transcription factors (TF), such as mRNA including *Zeb1/2*, *Twist1*, and *Snai1/2* (29). The EMT-TFs were inversely associated with the HER3 mRNA expression in the study cohort (Fig. 2B and D; Supplementary Fig. S3) as well as in TCGA lung adenocarcinoma cohort (Fig. 2C and D; Supplementary Fig. S3). In addition, the HER3 protein expression level positively correlated with the protein expression of the epithelial marker E-cadherin in TCGA lung adenocarcinoma cohort (Pearson,  $r = 0.4068$ ,  $P < 0.001$ ,  $n = 706$ ; Fig. 2E). We treated *EGFR*-mutated NSCLC PC9 cells with 4 ng/mL TGF $\beta$  for 10 days to determine whether the acquisition of mesenchymal features could alter the HER3 expression level. TGF $\beta$  increased the expression of the mesenchymal markers N-cadherin and vimentin, whereas E-cadherin and the HER3 expression level decreased (Fig. 2F). These results suggested that HER3 expression partially correlated with EMT, as reported previously (30); however, in tumors with *EGFR*-CNG, EMT-TF levels, except *SNAI1*, did not demonstrate augmentation despite the low HER3 expression compared with that in tumors without *EGFR*-CNG (Supplementary Fig. S4). Furthermore, GSEA could not detect an enrichment of gene sets related to EMT in tumors with *EGFR*-CNG compared with those without *EGFR*-CNG (Supplementary Fig. S5). Therefore, the augmentation of HER3 expression in tumors with *EGFR* mutation and CNG could be independent of the EMT process.

### HER3 augmentation after acquisition of EGFR-TKI resistance

We focused on the significant augmentation of HER3 expression in posttreatment samples compared with the pretreatment samples (Fig. 1H). We compared the clinical or genomic background between tumors with and without HER3 augmentation to identify the cause of HER3 augmentation; 56.2% (27/48) of all tumors showed an increased cell-surface HER3 expression in posttreatment samples compared with the pretreatment samples, and we divide tumor pairs into two groups: HER3 augmented group ( $n = 27$ ) and HER3 non-augmented group ( $n = 21$ ; Fig. 3A). Regardless of the causes of resistance, such as *EGFR* T790M mutation, *MET* amplification, *HER2* amplification, and histologically small cell lung cancer conversion, etc., HER3 augmentation was observed in the posttreatment samples (Fig. 3A and B). The HER3 augmentation did not obviously correlate with the type of EGFR-activating mutation (Pearson  $r = -0.007$ ,  $P = 0.961$ ), *EGFR* CNG in the posttreatment specimens (Pearson  $r = -0.057$ ,  $P = 0.706$ ), or the *EGFR* T790M mutation (Pearson  $r = 0.112$ ,  $P = 0.45$ ; Fig. 3A). The HER3 augmentation did not obviously correlate with clinical characteristics, such as smoking history, sex, type of EGFR-TKI



## HER3 Augmentation via Blockade of EGFR/AKT Signaling

**Figure 2.**

Relationship between HER3 expression and core EMT-TFs in EGFR-mutated NSCLC. **A**, A table of the hallmarks of gene sets observed in pretreatment samples with low HER3 expression compared to samples with high HER3 expression. Scatter plot analysis showing the relationship between HER3 mRNA and ZEB1/2 mRNA expression level in the current cohort (**B**, RNA-seq RSEM, TMM-normalized) or in TCGA lung adenocarcinoma dataset (**C**, RNA-seq RSEM, norm count+1). **D**, Relationship between HER3 mRNA and EMT-TFs mRNA including SNAI1/2, ZEB1/2, and TWIST1 mRNA expression level in the current cohort or TCGA lung adenocarcinoma dataset. **E**, Scatter plot analysis showing the relationship between HER3 protein expression and E-cadherin protein expression levels in TCGA lung adenocarcinoma dataset. Unit; RBM-normalized RPPA value. **F**, Immunoblotting analysis of indicated proteins from EGFR-mutated PC9 cells treated with 4 ng/mL of TGFβ for 10 days. NES, normalized enrichment score; NOM p-value, nominal p-value; FDR, false discovery rate; TCGA, The Cancer Genome Atlas; EGFR-TKI, epidermal growth factor receptor-tyrosine kinase inhibitor.

*CDK4/6*; 0.019, 0.909 for *p53*; **Fig. 3A**). In addition, the TMB in the posttreatment specimens showed no obvious correlation with altered HER3 expression levels (Pearson  $r = -0.153$ ,  $P = 0.299$ ; **Fig. 3A**).

**HER3 augmentation depending on PI3K/AKT/mTOR signaling**

To clarify the mechanisms underlying HER3 regulation in EGFR-mutated NSCLCs, we compared the transcriptomic features between HER3 augmented expression and HER3 non-augmented expression

groups. In the pretreatment specimens, there was no significant between-group difference in the hallmarks of the transcriptome (Supplementary Table S1). In the posttreatment specimens, gene sets related to EMT, such as TGFβ signaling and Wnt/β-catenin signaling, tended to be enriched in the HER3 augmented expression group compared with the HER3 non-augmented expression group (Supplementary Table S2). However, when we compared the expression level of EMT-TF mRNA, there was no significant difference between the



## HER3 Augmentation via Blockade of EGFR/AKT Signaling

**Table 1.** Hallmarks in pre- and posttreatment samples.

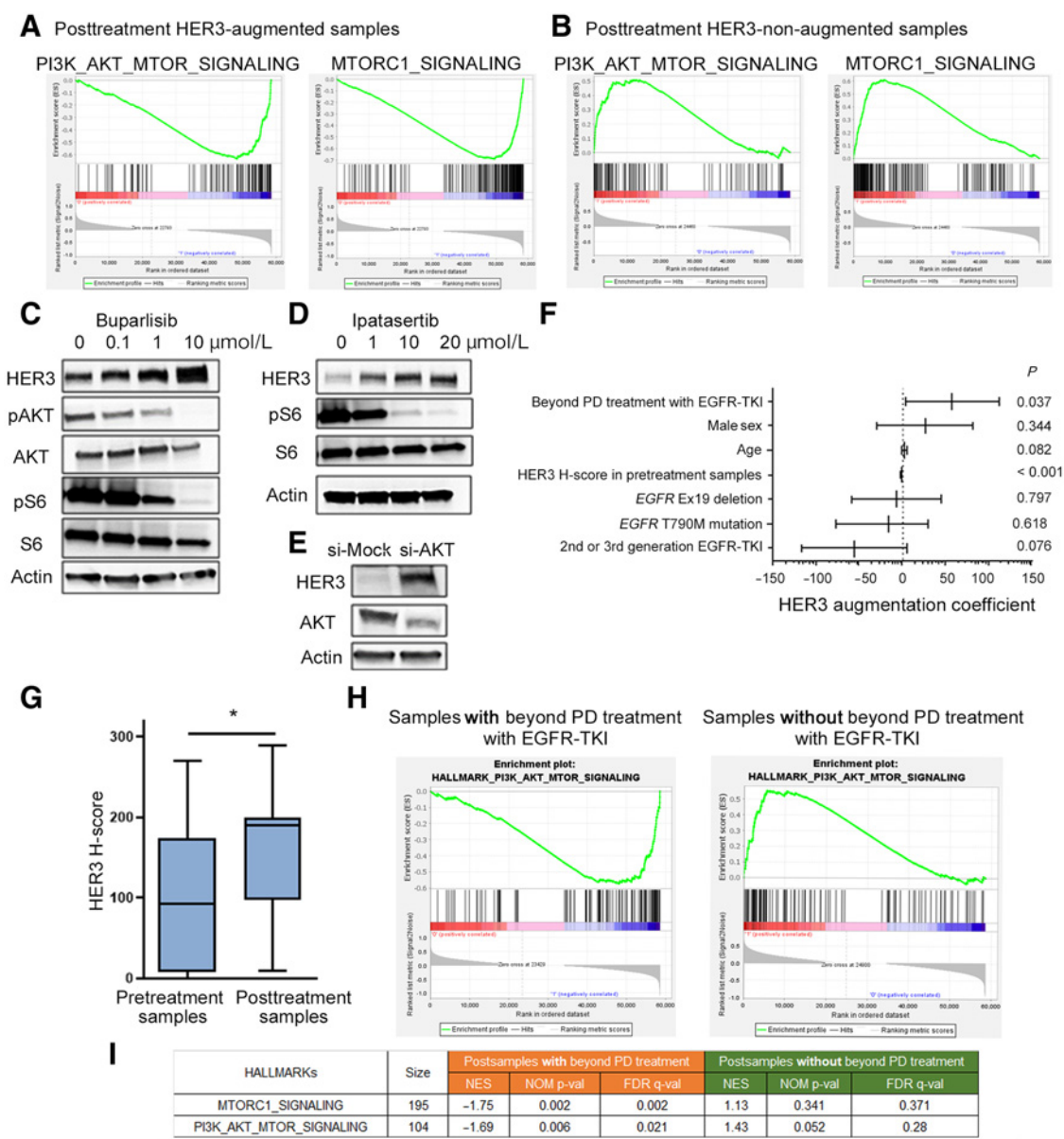
A. Posttreatment HER3 augmented samples, Posttreatment samples [vs. Pretreatment samples]					
RANK	HALLMRKS	SIZE	NES	NOM p-val	FDR q-val
1	HALLMARK_WNT_BETA_CATENIN_SIGNALING	42	-1.87	0.000	0.003
2	HALLMARK_UNFOLDED_PROTEIN_RESPONSE	107	-1.84	0.000	0.003
3	HALLMARK_PEROXISOME	104	-1.82	0.002	0.004
4	HALLMARK_ADIPOGENESIS	192	-1.81	0.000	0.004
5	HALLMARK_OXIDATIVE_PHOSPHORYLATION	184	-1.80	0.002	0.005
6	<b>HALLMARK_PI3K_AKT_MTOR_SIGNALING</b>	104	-1.78	0.004	0.006
7	HALLMARK_XENOBIOTIC_METABOLISM	198	-1.78	0.002	0.006
8	HALLMARK_DNA_REPAIR	147	-1.77	0.002	0.007
9	HALLMARK_FATTY_ACID_METABOLISM	156	-1.76	0.004	0.007
10	HALLMARK_REACTIVE_OXYGEN_SPECIES_PATHWAY	47	-1.75	0.002	0.007
11	<b>HALLMARK_MTORC1_SIGNALING</b>	195	-1.74	0.006	0.008
12	HALLMARK_ANDROGEN_RESPONSE	96	-1.72	0.004	0.009
13	HALLMARK_MITOTIC_SPINDLE	198	-1.72	0.008	0.008
14	HALLMARK_NOTCH_SIGNALING	32	-1.71	0.013	0.009
15	HALLMARK_ESTROGEN_RESPONSE_EARLY	196	-1.71	0.002	0.008
16	HALLMARK_ESTROGEN_RESPONSE_LATE	196	-1.71	0.002	0.008
17	HALLMARK_PROTEIN_SECRETION	95	-1.69	0.017	0.011
18	HALLMARK_GLYCOLYSIS	197	-1.67	0.010	0.014
19	HALLMARK_P53_PATHWAY	193	-1.66	0.006	0.016
20	HALLMARK_APICAL_JUNCTION	194	-1.66	0.019	0.015
B. Posttreatment HER3-augmented samples, Pretreatment samples [vs. Posttreatment samples]					
RANK	HALLMRKS	SIZE	NES	NOM p-val	FDR q-val
—	There is no gene set enriched.	—	—	—	—
C. Posttreatment HER3-non-augmented samples, Posttreatment samples [vs. Pretreatment samples]					
RANK	HALLMRKS	SIZE	NES	NOM p-val	FDR q-val
1	HALLMARK_HEME_METABOLISM	194	1.83	0.002	0.015
2	HALLMARK_CHOLESTEROL_HOMEOSTASIS	73	1.69	0.006	0.100
3	HALLMARK_COMPLEMENT	200	1.62	0.008	0.147
4	HALLMARK_DNA_REPAIR	147	1.59	0.040	0.153
5	HALLMARK_IL6_JAK_STAT3_SIGNALING	87	1.58	0.016	0.137
6	HALLMARK_REACTIVE_OXYGEN_SPECIES_PATHWAY	47	1.57	0.041	0.122
7	HALLMARK_P53_PATHWAY	193	1.54	0.032	0.140
8	HALLMARK_INFLAMMATORY_RESPONSE	199	1.54	0.018	0.123
9	<b>HALLMARK_MTORC1_SIGNALING</b>	195	1.52	0.082	0.136
10	HALLMARK_WNT_BETA_CATENIN_SIGNALING	42	1.52	0.032	0.122
11	HALLMARK_MITOTIC_SPINDLE	198	1.51	0.060	0.117
12	<b>HALLMARK_PI3K_AKT_MTOR_SIGNALING</b>	104	1.51	0.034	0.112
13	HALLMARK_UV_RESPONSE_UP	154	1.49	0.065	0.119
14	HALLMARK_GLYCOLYSIS	197	1.46	0.086	0.138
15	HALLMARK_OXIDATIVE_PHOSPHORYLATION	184	1.43	0.108	0.154
16	HALLMARK_IL2_STAT5_SIGNALING	195	1.40	0.060	0.176
17	HALLMARK_ALLOGRAFT_REJECTION	195	1.40	0.119	0.171
18	HALLMARK_ADIPOGENESIS	192	1.40	0.128	0.162
19	HALLMARK_PEROXISOME	104	1.39	0.098	0.159
20	HALLMARK_E2F_TARGETS	195	1.38	0.176	0.162
D. Posttreatment HER3-non-augmented samples, Pretreatment samples [vs. Posttreatment samples]					
RANK	HALLMRKS	SIZE	NES	NOM p-val	FDR q-val
1	HALLMARK_EPITHELIAL_MESENCHYMAL_TRANSITION	198	-0.90	0.554	0.969
2	HALLMARK_UV_RESPONSE_DN	139	-0.68	0.911	0.836

Abbreviations: FDR, false discovery rate; NES, normalized enrichment score; NOM p-value, nominal p-value.

pretreatment specimens, of the HER3 augmented expression group despite the fact that the tumors acquired resistance to EGFR-TKIs (Table 1; Fig. 4A). In contrast to the HER3-upregulated group, these gene sets were enriched in the posttreatment specimens, compared with the pretreatment specimens, of the HER3 non-augmented group (Table 1, Fig. 4B). We hypothesized that cell-surface HER3 expression could be regulated by PI3K/AKT/mTOR signaling and, therefore, we treated EGFR-mutated PC9 cells with the PI3K inhibitor buparlisib. Buparlisib decreased the phosphorylation of AKT and S6 but inversely increased HER3 expression in a dose-dependent manner (Fig. 4C).

Similarly, the AKT inhibitor ipatasertib decreased S6 phosphorylation but increased HER3 expression in a concentration-dependent manner (Fig. 4D). Furthermore, siRNA to specifically knockdown AKT expression increased HER3 protein expression in EGFR-mutated HCC827 cells compared with the siMock control (Fig. 4E). Given that PI3K/AKT/mTOR signaling activity influenced HER3 expression, there were several clinical or genomic factors, including the generation of EGFR-TKIs, EGFR secondary T790M mutations in posttreatment specimens, HER3 expression in the pretreatment specimens, type of EGFR-activating mutation, age, sex, and beyond PD treatment with

Yonesaka et al.

**Figure 4.**

Relationship between HER3 augmentation and PI3K/AKT/mTOR signaling in tumors. **A** and **B**, Representative GSEA plots of the MTORC1 signaling and PI3K/AKT/mTOR signaling gene signatures in the posttreatment HER3 augmented samples compared with the pretreatment samples (**A**), and in posttreatment HER3 non-augmented samples compared with pretreatment samples (**B**). Immunoblot analysis of indicated proteins from PC9 cells treated with the indicated concentrations of buparlisib (**C**) or ipatasertib (**D**) for 24 hours. **E**, Immunoblot analysis of several proteins from HCC827 cells transfected with siRNA against *AKT* or a non-targeting siRNA (siMock control). **F**, Multivariable regression analysis for HER3 augmentation with indicated variances. **G**, Box-and-whisker plot of the HER3 H-scores in pretreatment and posttreatment samples from subjects who were continuously treated with EGFR-TKI beyond PD. **H**, Representative GSEA plots of PI3K/AKT/mTOR signaling gene signature in posttreatment samples obtained from subjects with/without beyond PD treatment with EGFR-TKI compared with pretreatment samples. **I**, A table of the hallmarks of MTORC1 and PI3K/AKT/mTOR signaling obtained by GSEA in posttreatment samples harboring a T790M secondary EGFR mutation was obtained from participants with/without EGFR-TKI treatment beyond PD compared with that in the pretreatment samples. \*,  $P < 0.05$ , NES, normalized enrichment score; NOM p-value, nominal p-value; FDR, false discovery rate; PD, progressive disease.

EGFR-TKI, that potentially influenced PI3K/AKT/mTOR signaling activity. Multivariable regression analysis of HER3 augmentation using these factors revealed that rebiopsy under EGFR-TKI treatment independently effected HER3 augmentation (Fig. 4F). Twenty-eight patients continued to receive EGFR-TKIs to prevent a disease flare even after radiological confirmation of tumor progression, whereas 20

patients had discontinued EGFR-TKI treatment due to its toxicity and switched to other anticancer drugs (31). The HER3 H-score of the posttreatment specimen obtained from patients receiving EGFR-TKI treatment after PD was approximately 1.8 times greater than that of the pretreatment specimen (mean H-score 93.9 vs. 166,  $n = 26$ , paired  $t$  test  $P = 0.0028$ ; Fig. 4G). The HER3 H-score of the posttreatment

specimen from patients who did not receive EGFR-TKI treatment after PD was approximately 1.3 times greater than that of the pretreatment specimen (mean H-score 109.1 vs. 144.1,  $n = 22$ , paired  $t$  test  $P = 0.1029$ ). According to the transcriptional hallmark of posttreatment specimens obtained during EGFR-TKI treatment, gene sets related to MTORC1 or PI3K/AKT/mTOR signaling were significantly less enriched than those of pretreatment specimens, whereas posttreatment specimens free from EGFR-TKI treatment showed enrichment of these gene sets compared with pretreatment specimens (Fig. 4H). Furthermore, in a subpopulation with an acquired T790M secondary EGFR mutation, GSEA indicated that MTORC1 or PI3K/AKT/mTOR signaling was not active in posttreatment specimens obtained during EGFR-TKI therapy compared with that in pretreatment specimens; however, this signaling was activated in posttreatment specimens free from EGFR-TKI therapy compared with that in pretreatment specimens (Fig. 4I).

### HER3 augmentation via blockade of EGFR/AKT signaling enhancing the anticancer activity of HER3-DXd

To test whether an EGFR-TKI treatment could augment HER3 expression, EGFR-mutated NSCLC cells were treated with the EGFR-TKI osimertinib and the HER3 expression was evaluated *in vitro*. Five EGFR-mutated NSCLC lineage cells, including PC9, H1975, HCC827, HCC4006, and HCC827GR5 cells, showed increased HER3 expression during osimertinib treatment after 24 hours of treatment initiation regardless of the type of EGFR mutation, ex19 del, L858R, T790M, or concomitant MET amplification (Fig. 5A and B). Osimertinib inhibited EGFR phosphorylation and its downstream AKT phosphorylation in PC9 cells 3 hours after treatment (Fig. 5C). Moreover, other lineage cells showed decreased phosphorylation of EGFR and AKT 3 hours after osimertinib treatment (Fig. 5D). In addition to HER3 protein augmentation in whole cell lysates, HER3 mRNA level also increased in PC9 cells 24 hours after osimertinib treatment (Fig. 5E).

Here, we theorized that HER3 augmentation by EGFR-TKIs could enhance the anticancer activity of HER3-DXd; therefore, we tested this hypothesis using EGFR-mutated HCC827 cells and their clonal MET-amplified HCC827GR5 cells. The colony formation assay of HCC827 cells revealed a moderate anticancer activity of HER3-DXd and strong, but incomplete, activity of osimertinib (Fig. 5F). However, combination therapy with both HER3-DXd and osimertinib demonstrated near-complete anticancer activity in these cells (Fig. 5F). Furthermore, in HCC827GR5 cells, either HER3-DXd or osimertinib showed a moderate anticancer activity, but a combination of both drugs demonstrated significantly more potent activity than either drug alone (Fig. 5G). To elucidate the mechanism underlying the synergistic anticancer activity, we performed an immunoblotting assay using HCC827GR5 cells treated with HER3-DXd, osimertinib, and a combination of both drugs. HER3-DXd alone degraded HER3 and increased the phosphorylation of Histone H2A.X, a marker of DNA damage, leading to moderate PARP cleavage (Fig. 5H). However, combined treatment with HER3-DXd and osimertinib demonstrated greater phosphorylation of Histone H2A.X compared with HER3-DXd monotherapy (Fig. 5H). Finally, the combination of HER3-DXd and osimertinib resulted in more PARP cleavage than HER3-DXd or osimertinib monotherapy (Fig. 5H).

## Discussion

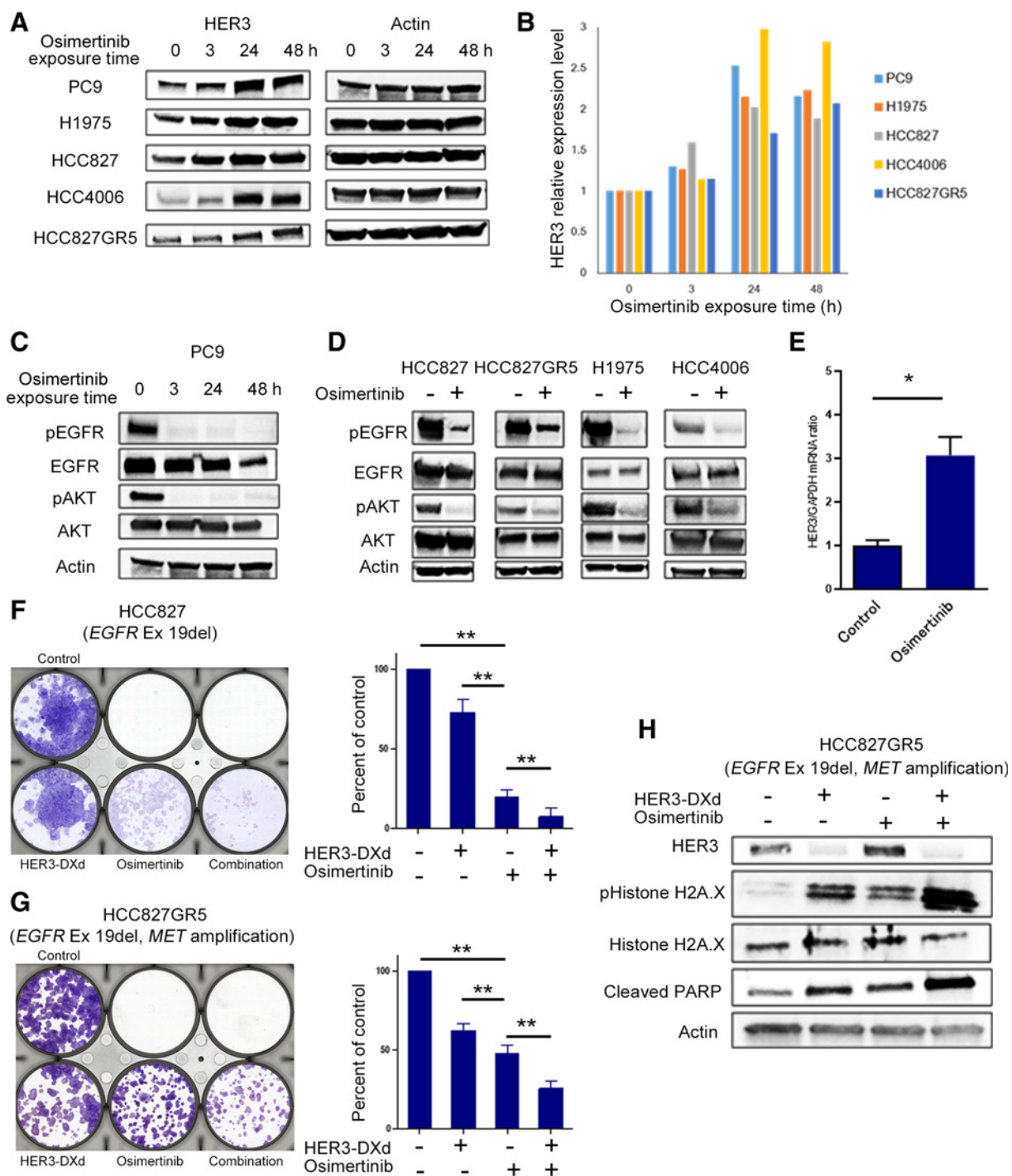
Here, we showed that EGFR-TKI treatment augmented the cell-surface HER3 expression in EGFR-mutated NSCLC tumors. Transcriptome analysis of tumors suggested that AKT inhibition by

EGFR-TKI caused a feedback-based HER3 augmentation that was validated in an *in vitro* study. Although HER3-DXd alone and the EGFR-TKI osimertinib alone had limited anticancer activity in MET-amplified and EGFR-mutated HCC827GR5 cells, exposure to osimertinib augmented the HER3 expression and thereby enhanced the anticancer activity of the HER3-DXd that was concomitantly administered. Our findings provide insights into mechanisms of HER3 regulation in EGFR-mutated NSCLC tumors and highlight the rationale for a combination therapy that is currently being evaluated in a clinical trial for patients with EGFR-mutated NSCLC tumors, not only with regard to an acquired resistance to EGFR-TKI but also in EGFR-TKI-naïve tumors (NCT04676477; ref. 32).

HER3 was previously known to be frequently expressed in some kinds of cancer, including EGFR-mutated NSCLC, whereas HER3 augmentation was not evident in tumors treated with EGFR-TKIs (14, 16). However, the findings from an *in vitro* study for breast cancer suggested that HER3 expression could be potentially augmented by anticancer treatments through signaling blockade (33). Thus, Sergina and colleagues reported that TKIs acted against the HER family to increase the cell-membrane HER3 expression that was driven by the cessation of AKT-mediated negative-feedback signaling in HER2-positive breast cancer cells (33). Those authors suggested that HER3 was largely pooled within intracellular compartments in these cells, whereas HER3 relocated to the cell membrane after a TKI exposure and was phosphorylated by a residual HER2 kinase activity, which led to an escape from the proapoptotic effects of TKIs (33, 34). In addition, our previous study using osimertinib-resistant EGFR-mutated NSCLC PC9AZDR7 cells showed an increased HER3 expression on the cell membrane whereas there was a decreased HER3 expression in the cell nucleus when compared to observations in the parent PC9 cells (23). Considering these results, EGFR-mutated tumors could carry abundant intracellular HER3 proteins that relocate to the cell surface after the inhibition of AKT signaling by EGFR-TKI treatment. However, it is difficult for EGFR-TKI to completely extinguish EGFR kinase activity in tumors, presumably due to intratumoral heterogeneity and as HER3 could be phosphorylated by residual EGFR activity in tumors treated with EGFR-TKI (35). Indeed, Haikala and colleagues reported that HER3 coupled with EGFR was augmented in EGFR-mutated cancer cells treated with EGFR-TKIs in *in vitro* and *in vivo* studies (36). Alternatively, HER3 could be phosphorylated dependently on ligands, especially heregulin, which induced coupling with HER2 (18, 37). Paracrine heregulin production by stromal cells or autocrine production by cancer cells was reported to play a role in the activation of HER3 in tumors (38). Collectively, cell-surface HER3 augmentation and its assumed phosphorylation by residual EGFR activity or by HER2 potentially contributed to the tumor's tolerance to EGFR-TKIs in tumors that were treated previously with EGFR-TKIs. Inversely, EGFR genomic amplification could potentially lead to excessively activated EGFR-AKT signaling and, in turn, repress cell-surface HER3 expression in EGFR-mutated NSCLC tumors. By establishing a balance between HER3 and activated EGFR expression for maintaining AKT signaling, EGFR-mutated tumors could maintain anti-apoptosis in varying environments or under an EGFR-TKI treatment.

Alternatively, HER3 expression might be regulated in an MYC-dependent transcriptional manner even in EGFR-mutated NSCLC. A human core promoter microarray identified 1,469 MYC direct-binding target genes; HER3 was included in these genes, which suggested that it could be regulated by MYC (39). In addition, knockdown of MYC induced the expression of several receptors including HER3, suggesting that MYC potentially represses HER3

Yonesaka et al.

**Figure 5.**

HER3 augmentation induced by EGFR-TKI that enhanced the anticancer activity of HER3-DXd. **A** and **B**, Immunoblot analysis of HER3 and actin from EGFR-mutated NSCLC cells treated with 100 nmol/L osimertinib for the indicated duration. The level of HER3 expression was measured and quantified using Image J (**B**). Y-axis, fold changes compared with the untreated control of an individual cell. Immunoblot analysis of indicated proteins from EGFR-mutated NSCLC cells treated with 100 nmol/L osimertinib for the indicated duration (**C**) or 3 hours (**D**). **E**, HER3 mRNA expression was quantitatively analyzed by PCR with GAPDH normalization in PC9 cells treated with 100 nmol/L osimertinib for 24 hours (mean  $\pm$  SD of four independent experiments). **F** and **G**, Clonogenic assay for EGFR-mutated HCC827 (**F**) and its clonal *MET*-amplified HCC827GR5 cells (**G**) treated with/without 3  $\mu$ g/mL HER3-DXd, 100 nmol/L osimertinib alone, or a combination of both drugs for 10 days. The colony formation area was measured and quantified using Image J, and the measurement was repeated three times. Y-axis, fold changes compared with the untreated control. **H**, Immunoblot analysis of the indicated proteins from HCC827GR5 cells treated with/without 3  $\mu$ g/mL HER3-DXd, 100 nmol/L osimertinib alone, or a combination of both drugs for 5 days. \*,  $P < 0.05$ , unpaired *t* test; \*\*,  $P < 0.05$ , Dunnett multiple comparison test. Both **A** and **C** show the same actin blot because they were from the same samples.

expression (40). GSEA showed that samples with *EGFR* CNG had a gene signature of MYC activation, suggesting that HER3 might be repressed in a MYC-dependent manner (Supplementary Fig. S5). Inversely, EGFR-TKI treatment inactivated the MYC pathway in posttreatment specimens compared with pretreatment specimens (Supplementary Table S3). According to previous reports, MYC could be regulated by multiple pathways and, indeed, EGFR-mutated NSCLC tumors revealed altered Wnt/ $\beta$ -catenin signaling, TGF $\beta$  signaling, and PI3K/AKT/mTOR signaling following EGFR-TKI treatment, which may have induced MYC-dependent HER3 augmentation (Supplementary Table S3; ref. 41). In addition, multiple and putative pathways, including FOXOs, CTBP1/CTBP2, and miRNAs, were reported to regulate HER3 expression in *in vitro* studies (42–45). However, the current study could not identify a significant relationship of these gene expressions with HER3 expression, or conceivably implied that HER3 augmentation might be regulated via multiple pathways in EGFR-mutated NSCLC tumors, in contrast to the mechanism identified in *in vitro* studies. Previous studies have indicated that the maintenance of PI3K signaling was critical for survival in EGFR-mutated NSCLC cells, especially by inducing resistance to EGFR-TKIs (8, 46). Until the development of secondary mutations, such as *EGFR*, *PIK3CA*, and *MET* amplification, HER3 augmentation that is mediated by multiple pathways was assumed to temporally direct cells toward acquiring EGFR-TKI tolerance through activated HER3/PI3K/AKT signaling.

HER3 augmentation after the acquisition of EGFR-TKI resistance was observed in EGFR-mutated NSCLC tumors regardless of the type of mechanisms underlying the EGFR-TKI resistance, such as EGFR T790M mutation, *MET* amplification, and HER2 amplification. Especially in tumors that acquired a resistance to EGFR-TKI based on EGFR T790M, the AKT signals were inhibited by EGFR-TKI, whereby HER3 could be augmented. These results suggested that some tumors depend on EGFR for maintaining AKT signaling even after acquiring resistance to EGFR-TKIs. In clinical practice, a rapid tumor progression would occasionally occur after the cessation of EGFR-TKI treatment—the so-called disease flare (31). Chaft and colleagues reported that 14 of 61 patients (23%) experienced a disease flare after the cessation of EGFR-TKI treatment (31). In addition, their investigation showed no association between disease flare and the presence of T790M at the time of acquired resistance (31). When considering the results of Chaft and colleagues with the results of our study, we infer that AKT inhibition by EGFR-TKI maintains the proapoptotic capability of EGFR-mutated tumors despite clinical or radiological progression. Furthermore, the elimination of AKT inhibition by stopping EGFR-TKI treatment potentially induces a disease flare. Our results support the advantage of EGFR-TKI beyond PD therapy or its combination with other agents, especially HER3-DXd. Alternatively, the EGFR-TKI resistance could be achieved via other signaling pathways, such as RAF/MEK/ERK signaling or EMT (47). Ercan and colleagues reported that resistance to EGFR inhibitors can also arise through persistent or reactivated ERK1/2 signaling (47). Some HER3-augmented tumors had genomic mutations in the RAF/MEK/ERK pathway, and *DUSP1* expression decreased by approximately 50% in posttreatment specimens compared with pretreatment specimens (mean value 160.0 vs. 81.8, unpaired *t* test  $P = 0.018$ ), which might be related to ERK-mediated resistance.

Previous HER3-targeting strategies were predominantly dependent on signaling blockade of the HER3/PI3K/AKT axis but could not necessarily provide significant efficacy in clinical trials of NSCLC (18, 48, 49). One reason for this limitation is the insufficient anticancer activity induced by cell signaling blockade alone or a

technically incomplete blockade of HER3 signaling (18). HER3-DXd resolved this limitation by selective drug delivery and potent DNA damage (19, 22, 23). Indeed, HER3-DXd demonstrated superior anticancer activity in early-phase clinical trials although the subjects were heavily pretreated with EGFR-TKIs and other chemotherapies (25). The anticancer activity of ADCs partly depends on the expression level of the antigen and, indeed, the HER2-targeting ADC trastuzumab deruxtecan, which possesses the same linker-payload system as HER3-DXd, demonstrated excellent anticancer activity, especially for HER2-amplified cancers (19). Alternatively, an increased dosage might provide more potent anticancer efficacy but simultaneously induce more toxicity. Therefore, cell-surface HER3 augmentation in tumors could be a critical solution for enhancing the anticancer activity of HER3-DXd without inducing toxicity. In this context, the results of our study suggested that combination therapy with EGFR-TKI and HER3-DXd might be superior to HER3-DXd monotherapy for treating EGFR-mutated NSCLC. In addition, this strategy might resolve not only the limitation of second-line therapy for an acquired resistance to EGFR-TKI but also supplement a weak advantage with first-line EGFR-TKI therapy in EGFR-mutated NSCLC. Thus, the third-generation EGFR-TKI osimertinib demonstrated superior anticancer efficacy than first-generation EGFR-TKIs, whereas tumor heterogeneity induced resistance to osimertinib and limited the duration of its efficacy (3). This study revealed an HER3 augmentation across multiple tumors after the acquisition of EGFR-TKI resistance regardless of the causes of resistance. Therefore, a concomitant HER3-targeting strategy with HER3-DXd and EGFR-TKI might resolve the limitations of first-line EGFR-TKI therapy. In accordance with this strategy, a clinical trial is ongoing to evaluate combination therapy with osimertinib and HER3-DXd in EGFR-mutated NSCLC not only in participants with acquired resistance to EGFR-TKI but also in those who are EGFR-TKI naïve (32).

Thus, EGFR-TKI can inhibit pathways such as MAPK or STAT3; the status of these pathways may influence HER3 expression. However, the gene set of MEK activation was not significantly repressed in tumors with HER3 augmentation (normalized enrichment scores =  $-1.27$ , nominal  $P = 0.15$ ). Moreover, the MEK inhibitor trametinib did not alter HER3 expression in EGFR-mutated NSCLC PC9 cells, although the decrease in ERK phosphorylation was dependent on drug concentration (Supplementary Fig. S7). In addition, the levels of PTEN protein expression may influence AKT activity and HER3 expression, which may influence HER3-DXd activity. The limited cell line panel used in this study or previously (23) could not recapitulate the full spectrum of NSCLC phenotypes harboring the mutated *EGFR*, particularly those with sensitivity to HER3-DXd; therefore, our novel hypothesis requires further examination in clinical studies involving HER3-DXd that explore the optimal biomarkers for EGFR-mutated NSCLC. In conclusion, HER3 expression was further augmented in posttreatment EGFR-mutated NSCLC tumor specimens than in pretreatment specimens; this augmentation was likely mediated by PI3K/AKT/mTOR signaling. Thus, HER3 augmentation may enhance the anticancer activity of HER3-DXd.

#### Authors' Disclosures

K. Yonesaka reports grants from Daiichi Sankyo Co., Ltd. during the conduct of the study as well as personal fees from Boehringer Ingelheim outside the submitted work; in addition, K. Yonesaka has a patent for US20200115467 pending and a patent for US20200061031 pending. J. Tanizaki reports personal fees from AstraZeneca K.K., Boehringer-Ingelheim Japan Inc., Bristol-Myers Squibb Co. Ltd., Chugai Pharmaceutical Co. Ltd., Eli Lilly Japan K.K., MSD K.K., and Taiho

## Yonesaka et al.

Pharmaceutical Co. Ltd. outside the submitted work. K. Haratani reports personal fees from AS ONE Corporation, Bristol-Myers Squibb Co. Ltd., Chugai Pharmaceutical Co. Ltd., and Ono Pharmaceutical Co. Ltd. and grants and personal fees from AstraZeneca K.K. and MSD K.K. outside the submitted work. H. Kawakami reports personal fees from Daiichi-Sankyo Co. Ltd. during the conduct of the study as well as grants and personal fees from Bristol-Myers Squibb Co. Ltd. and Taiho Pharmaceutical Co. Ltd.; personal fees from Eli Lilly Japan K.K., MSD K.K., Ono Pharmaceutical Co. Ltd., Chugai Pharmaceutical Co. Ltd., Merck Biopharma Co., Ltd., Takeda Pharmaceutical Co. Ltd., and Yakult Pharmaceutical Industry; and grants from Kobayashi Pharmaceutical Co., Ltd. and Eisai Co. Ltd. outside the submitted work. K. Tanaka reports personal fees from Merck Biopharma, AstraZeneca, Eisai, Bristol-Myers Squibb, Ono Pharmaceutical, MSD, and Kyowa Kirin outside the submitted work. H. Hayashi reports personal fees from AstraZeneca K.K., Boehringer Ingelheim Japan Inc., Bristol-Myers Squibb Co. Ltd., Chugai Pharmaceutical Co. Ltd., Eli Lilly Japan K.K., Kyorin Pharmaceutical Co. Ltd., Merck Biopharma Co., Ltd., MSD K.K., Novartis Pharmaceuticals K.K., Ono Pharmaceutical Co. Ltd., Shanghai Haihe Biopharm, Taiho Pharmaceutical Co. Ltd., and Takeda Pharmaceutical Company Limited and grants from AstraZeneca K.K., Boehringer Ingelheim Japan Inc., Bristol-Myers Squibb Co. Ltd., Chugai Pharmaceutical Co. Ltd., Eli Lilly Japan K.K., Pfizer Japan Inc., Shanghai Haihe Biopharm, Takeda Pharmaceutical Company Limited, and Merck Biopharma Co., Ltd. outside the submitted work. K. Sakai reports personal fees from Roche Diagnostics, Bio-Rad, AstraZeneca, Chugai Pharma, and Hitachi outside the submitted work. Y. Hashimoto reports personal fees from Daiichi Sankyo Co., Ltd. during the conduct of the study. K. Hirotani reports other support from Daiichi Sankyo Co., Ltd. during the conduct of the study. T. Kagari reports other support from Daiichi Sankyo Co., Ltd. during the conduct of the study. K. Nishio reports grants from Nippon Boehringer Ingelheim, West Japan Oncology Group, Ignyta, Inc., Korea Otsuka Pharmaceutical, Eli Lilly, Thoracic Oncology Research Group, North East Japan Study Group, Clinical Research Support Center Kyushu, Nichirei Biosciences Inc., and Osakaminami Hospital and personal fees from Symbio Pharmaceuticals, Solasia Pharma, Eli Lilly Japan, Otsuka Pharmaceutical, Chugai, Eisai, Pfizer, Boehringer Ingelheim Japan, Novartis Pharma, MSD, Ono Pharmaceutical, Bristol-Myers Squibb, Life Technologies Japan, Yakult Honsha, Roche Diagnostics, AstraZeneca, Sanofi, Guardant Health, Amgen, and Merck Biopharma outside the submitted work. K. Nakagawa reports grants and personal fees from AstraZeneca K.K., MSD K.K., Nippon Boehringer Ingelheim Co., Ltd., Novartis Pharma K.K., Bristol Myers Squibb Company, Chugai Pharmaceutical Co., Ltd., Daiichi Sankyo Co., Ltd., Merck Biopharma Co., Ltd., AbbVie Inc, Kyowa Kirin Co., Ltd, Bayer Yakuhin, Ltd. and grants, personal fees, and other support from Astellas Pharma Inc., Ono Pharmaceutical Co., Ltd., Pfizer Japan Inc., and Eli Lilly Japan K.K. during the conduct of the study as well as personal fees from Medicus Shuppan, Publishers Co., Ltd., Care Net, Inc, Medical Review Co., Ltd., Roche

Diagnostics K.K., Medical Mobile Communications Co., Ltd, H Clinical Trial Inc., Nichi-Iko Pharmaceutical Co., Ltd., Yodosha Co., Ltd., Nikkei Business Publications, Inc, Thermo Fisher Scientific K.K., Yomiuri Telecasting Corporation, Nippon Kayaku Co., Ltd., Hisamitsu Pharmaceutical Co., Inc., Nanzando Co., Ltd, and Amgen Inc.; personal fees and other support from Kyorin Pharmaceutical Co., Ltd.; grants, personal fees, and other support from Takeda Pharmaceutical Co., Ltd.; and grants and personal fees from Taiho Pharmaceutical Co., Ltd., Symbio Pharmaceuticals Limited; grants from Icon Japan K.K., Parexel International Corp., Kissei Pharmaceutical Co., Ltd., EPS Corporation, Syneos Health, Pfizer R&D Japan G.K., A2 Healthcare Corp., Iqvia Services Japan K.K., Eisai Co., Ltd., CMIC Shift Zero K.K., EPS International Co., Ltd., Otsuka Pharmaceutical Co., Ltd., PRA Healthsciences, Covance Japan Inc., Medical Reserch Support, Sanofi K.K., PPD-SNBL K.K., Japan Clinical Research Operations, Sysmex Corporation, Mochida Pharmaceutical Co., Ltd., and GlaxoSmithKline K.K. outside the submitted work. No disclosures were reported by the other authors.

### Authors' Contributions

**K. Yonesaka:** Conceptualization, resources, funding acquisition, investigation, writing—original draft, writing—review and editing. **J. Tanizaki:** Resources. **O. Maenishi:** Investigation, methodology. **K. Haratani:** Resources. **H. Kawakami:** Resources. **K. Tanaka:** Resources. **H. Hayashi:** Resources. **K. Sakai:** Data curation, software, formal analysis, writing—review and editing. **Y. Chiba:** Formal analysis, writing—review and editing. **A. Tsuya:** Resources. **H. Goto:** Data curation, investigation. **E. Otsuka:** Data curation, investigation. **H. Okida:** Data curation, investigation. **M. Kobayashi:** Data curation, investigation. **R. Yoshimoto:** Data curation, investigation. **M. Funabashi:** Data curation, supervision, investigation, writing—review and editing. **Y. Hashimoto:** Supervision, project administration. **K. Hirotani:** Project administration. **T. Kagari:** Supervision, project administration. **K. Nishio:** Supervision. **K. Nakagawa:** Supervision, funding acquisition.

### Acknowledgments

This study was financially supported by Daiichi Sankyo Co., Ltd. We thank Junichi Okutsu, Mami Kitano, Haruka Sakamoto, Yume Shinkai, and Michiko Kitano for technical support.

The costs of publication of this article were defrayed in part by the payment of page charges. This article must therefore be hereby marked *advertisement* in accordance with 18 U.S.C. Section 1734 solely to indicate this fact.

Received September 17, 2021; revised November 4, 2021; accepted November 22, 2021; published first December 17, 2021.

### References

- Mitsudomi T, Morita S, Yatabe Y, Negoro S, Okamoto I, Tsurutani J, et al. Gefitinib versus cisplatin plus docetaxel in patients with non-small-cell lung cancer harbouring mutations of the epidermal growth factor receptor (WJTOG3405): an open label, randomised phase 3 trial. *Lancet Oncol* 2010; 11:121–8.
- Paz-Ares L, Tan E-H, O'Byrne K, Zhang L, Hirsh V, Boyer M, et al. Afatinib versus gefitinib in patients with EGFR mutation-positive advanced non-small-cell lung cancer: overall survival data from the phase IIb LUX-Lung 7 trial. *Ann Oncol* 2017;28:270–7.
- Popat S. Osimertinib as first-line treatment in EGFR-mutated non-small-cell lung cancer. *N Engl J Med* 2018;378:192–3.
- Rebuzzi SE, Alfieri R, La Monica S, Minari R, Petroni PG, Tiseo M. Combination of EGFR-TKIs and chemotherapy in advanced EGFR mutated NSCLC: Review of the literature and future perspectives. *Crit Rev Oncol Hematol* 2020; 146:102820.
- Kobayashi S, Boggon TJ, Dayaram T, Jänne PA, Kocher O, Meyerson M, et al. EGFR mutation and resistance of non-small-cell lung cancer to gefitinib. *N Engl J Med* 2005;352:786–92.
- Sequist LV, Waltman BA, Dias-Santagata D, Digumarthy S, Turke AB, Fidias P, et al. Genotypic and histological evolution of lung cancers acquiring resistance to EGFR inhibitors. *Sci Transl Med* 2011;3:75ra26.
- Thress KS, Pawelcz CP, Felip E, Cho BC, Stetson D, Dougherty B, et al. Acquired EGFR C797S mutation mediates resistance to AZD9291 in non-small cell lung cancer harboring EGFR T790M. *Nat Med* 2015;21:560–2.
- Engelman JA, Zejnullahu K, Mitsudomi T, Song Y, Hyland C, Park JO, et al. MET amplification leads to gefitinib resistance in lung cancer by activating ERBB3 signaling. *Science* 2007;316:1039–43.
- Takezawa K, Pirazzoli V, Arcila ME, Nebhan CA, Song X, de Stanchina E, et al. HER2 amplification: a potential mechanism of acquired resistance to EGFR inhibition in EGFR-mutant lung cancers that lack the second-site EGFR T790M mutation. *Cancer Discov* 2012;2:922–33.
- Zhou C, Yao LD. Strategies to improve outcomes of patients with EGFR-mutant non-small cell lung cancer: review of the literature. *J Thorac Oncol* 2016;11:174–86.
- Jia Y, Yun C-H, Park E, Ercan D, Manuia M, Juarez J, et al. Overcoming EGFR (T790M) and EGFR(C797S) resistance with mutant-selective allosteric inhibitors. *Nature* 2016;534:129–32.
- Sequist LV, Han J-Y, Ahn M-J, Cho BC, Yu H, Kim S-W, et al. Osimertinib plus savolitinib in patients with EGFR mutation-positive, MET-amplified, non-small-cell lung cancer after progression on EGFR tyrosine kinase inhibitors: interim results from a multicentre, open-label, phase 1b study. *Lancet Oncol* 2020;21:373–86.
- Wu Y-L, Cheng Y, Zhou J, Lu S, Zhang Y, Zhao J, et al. Tepotinib plus gefitinib in patients with EGFR-mutant non-small-cell lung cancer with MET overexpression or MET amplification and acquired resistance to previous EGFR inhibitor (INSIGHT study): an open-label, phase 1b/2, multicentre, randomised trial. *Lancet Respir Med* 2020;8:1132–43.
- Haikala HM, Jänne PA. Thirty years of HER3: from basic biology to therapeutic interventions. *Clin Cancer Res* 2021;27:3528–39.

## HER3 Augmentation via Blockade of EGFR/AKT Signaling

15. Yi ES, Harclerode D, Gondo M, Stephenson M, Brown RW, Younes M, et al. High c-erbB-3 protein expression is associated with shorter survival in advanced non-small cell lung carcinomas. *Mod Pathol* 1997;10:142–8.
16. Kawakami H, Yonesaka K. HER3 and its ligand, heregulin, as targets for cancer therapy. *Recent Pat Anticancer Drug Discov* 2016;11:267–74.
17. Engelman JA, Janne PA, Mermel C, Pearlberg J, Mukohara T, Fleet C, et al. ErbB-3 mediates phosphoinositide 3-kinase activity in gefitinib-sensitive non-small cell lung cancer cell lines. *Proc Natl Acad Sci U S A* 2005;102:3788–93.
18. Yonesaka K, Hirotsu K, Kawakami H, Takeda M, Kaneda H, Sakai K, et al. Anti-HER3 monoclonal antibody patritumab sensitizes refractory non-small cell lung cancer to the epidermal growth factor receptor inhibitor erlotinib. *Oncogene* 2016;35:878–86.
19. Yonesaka K. HER2-/HER3-targeting antibody-drug conjugates for treating lung and colorectal cancers resistant to EGFR inhibitors. *Cancers* 2021;13:1047.
20. Doi T, Shitara K, Naito Y, Shimomura A, Fujiwara Y, Yonemori K, et al. Safety, pharmacokinetics, and antitumor activity of trastuzumab deruxtecan (DS-8201), a HER2-targeting antibody-drug conjugate, in patients with advanced breast and gastric or gastro-oesophageal tumours: a phase 1 dose-escalation study. *Lancet Oncol* 2017;18:1512–22.
21. Tamura K, Tsurutani J, Takahashi S, Iwata H, Krop IE, Redfern C, et al. Trastuzumab deruxtecan (DS-8201a) in patients with advanced HER2-positive breast cancer previously treated with trastuzumab emtansine: a dose-expansion, phase 1 study. *Lancet Oncol* 2019;20:816–26.
22. Hashimoto Y, Koyama K, Kamai Y, Hirotsu K, Ogitani Y, Zembutsu A, et al. A novel HER3-targeting antibody-drug conjugate, U3-1402, exhibits potent therapeutic efficacy through the delivery of cytotoxic payload by efficient internalization. *Clin Cancer Res* 2019;25:7151–61.
23. Yonesaka K, Takegawa N, Watanabe S, Haratani K, Kawakami H, Sakai K, et al. An HER3-targeting antibody-drug conjugate incorporating a DNA topoisomerase I inhibitor U3-1402 conquers EGFR tyrosine kinase inhibitor-resistant NSCLC. *Oncogene* 2019;38:1398–409.
24. Koganemaru S, Kuboki Y, Koga Y, Kojima T, Yamauchi M, Maeda N, et al. U3-1402, a novel HER3-targeting antibody-drug conjugate, for the treatment of colorectal cancer. *Mol Cancer Ther* 2019;18:2043–50.
25. Janne PA, Baik CS, Su W-C, Johnson ML, Hayashi H, Nishio M, et al. Efficacy and safety of patritumab deruxtecan (HER3-DXd) in EGFR inhibitor-resistant, EGFR-mutated (EGFR m) non-small cell lung cancer (NSCLC). *J Clin Oncol* 39: 15s, 2021 (suppl; abstr 9007).
26. Janne P, Baik C, Hayashi H, Su W, Qi Z, Enomoto K, et al. Dynamics of molecular markers in EGFR-mutated NSCLC patients treated with patritumab deruxtecan (HER3-DXd; U3-1402). *J Thorac Oncol* 2021;16.3:S237.
27. Goldman MJ, Craft B, Hastie M, Repecka K, McDade F, Kamath A, et al. Visualizing and interpreting cancer genomics data via the Xena platform. *Nat Biotechnol* 2020;38:675–8.
28. Shi J, Walker MG. Gene set enrichment analysis (GSEA) for interpreting gene expression profiles. *Curr Bioinform* 2007;2.2:133–7.
29. Yang J, Antin P, Bex G, Blanpain C, Brabletz T, Bronner M, et al. Guidelines and definitions for research on epithelial-mesenchymal transition. *Nat Rev Mol Cell Biol* 2020;21:341–52.
30. Kitai H, Ebi H, Tomida S, Floros KV, Kotani H, Adachi Y, et al. Epithelial-to-mesenchymal transition defines feedback activation of receptor tyrosine kinase signaling induced by MEK inhibition in KRAS-mutant lung cancer. *Cancer Discov* 2016;6:754–69.
31. Chaff JE, Oxnard GR, Sima CS, Kris MG, Miller VA, Riely GJ. Disease flare after tyrosine kinase inhibitor discontinuation in patients with EGFR-mutant lung cancer and acquired resistance to erlotinib or gefitinib: implications for clinical trial design. *Clin Cancer Res* 2011;17:6298–303.
32. Janne P, Rajagopalan R, Pudussery G, Shrestha P, Chen S, Hodge R, et al. Phase 1 study of patritumab deruxtecan (HER3-DXd; U3-1402) in combination with osimertinib in patients with locally advanced or metastatic EGFR-mutated NSCLC. *J Thorac Oncol* 2021;16.3:S237.
33. Sergina NV, Rausch M, Wang D, Blair J, Hann B, Shokat KM, et al. Escape from HER-family tyrosine kinase inhibitor therapy by the kinase-inactive HER3. *Nature* 2007;445:437–41.
34. Offjerdinger M, Schöfer C, Weipoltshammer K, Grunt TW. c-erbB-3: a nuclear protein in mammary epithelial cells. *J Cell Biol* 2002;157:929–39.
35. Soucheray M, Capelletti M, Pulido I, Kuang Y, Pawletz CP, Becker JH, et al. Intratumoral heterogeneity in EGFR-mutant NSCLC results in divergent resistance mechanisms in response to EGFR tyrosine kinase inhibition. *Cancer Res* 2015;75:4372–83.
36. Haikala HM, Lopez T, Köhler J, Eser PO, Xu M, Zeng Q, et al. EGFR inhibition enhances the cellular uptake and antitumor-activity of the HER3 antibody drug conjugate HER3-DXd. *Cancer Res* 2021 Sep 21 [Epub ahead of print].
37. Yonesaka K, Kudo K, Nishida S, Takahama T, Iwasa T, Yoshida T, et al. The pan-HER family tyrosine kinase inhibitor afatinib overcomes HER3 ligand heregulin-mediated resistance to EGFR inhibitors in non-small cell lung cancer. *Oncotarget* 2015;6:33602–11.
38. Zhang Z, Karthaus WR, Lee YS, Gao VR, Wu C, Russo JW, et al. Tumor microenvironment-derived NRG1 promotes antiandrogen resistance in prostate cancer. *Cancer Cell* 2020;38:279–96.
39. Duncan JS, Whittle MC, Nakamura K, Abell AN, Midland AA, Zawistowski JS, et al. Dynamic reprogramming of the kinome in response to targeted MEK inhibition in triple-negative breast cancer. *Cell* 2012;149:307–21.
40. Sun C, Hobor S, Bertotti A, Zecchin D, Huang S, Galimi F, et al. Intrinsic resistance to MEK inhibition in KRAS mutant lung and colon cancer through transcriptional induction of ERBB3. *Cell Rep* 2014;7:86–93.
41. Dang CV. MYC on the path to cancer. *Cell* 2012;149:22–35.
42. Chakrabarty A, Sánchez V, Kuba MG, Rinehart C, Arteaga CL. Feedback upregulation of HER3 (ErbB3) expression and activity attenuates antitumor effect of PI3K inhibitors. *Proc Natl Acad Sci U S A* 2012;109:2718–23.
43. Garrett JT, Olivares MG, Rinehart C, Granja-Ingram ND, Sanchez V, Chakrabarty A, et al. Transcriptional and posttranslational up-regulation of HER3 (ErbB3) compensates for inhibition of the HER2 tyrosine kinase. *Proc Natl Acad Sci U S A* 2011;108:5021–6.
44. Montero-Conde C, Ruiz-Llorente S, Dominguez JM, Knauf JA, Viale A, Sherman EJ, et al. Relief of feedback inhibition of HER3 transcription by RAF and MEK inhibitors attenuates their antitumor effects in BRAF-mutant thyroid carcinomas. *Cancer Discov* 2013;3:520–33.
45. Iorio MV, Casalini P, Piovano C, Di Leva G, Merlo A, Triulzi T, et al. microRNA-205 regulates HER3 in human breast cancer. *Cancer Res* 2009;69:2195–200.
46. Engelman JA, Mukohara T, Zejnullahu K, Lifshits E, Borras AM, Gale C-M, et al. Allelic dilution obscures detection of a biologically significant resistance mutation in EGFR-amplified lung cancer. *J Clin Invest* 2006;116:2695–706.
47. Ercan D, Xu C, Yanagita M, Monast CS, Pratilas CA, Montero J, et al. Reactivation of ERK signaling causes resistance to EGFR kinase inhibitors. *Cancer Discov* 2012;2:934–47.
48. Shimizu T, Yonesaka K, Hayashi H, Iwasa T, Haratani K, Yamada H, et al. Phase 1 study of new formulation of patritumab (U3-1287) Process 2, a fully human anti-HER3 monoclonal antibody in combination with erlotinib in Japanese patients with advanced non-small cell lung cancer. *Cancer Chemother Pharmacol* 2017;79:489–95.
49. Sequist LV, Janne PA, Huber RM, Gray JE, Felip E, Perol M, et al. SHERLOC: A phase 2 study of MM-121 plus with docetaxel versus docetaxel alone in patients with heregulin (HRG) positive advanced non-small cell lung cancer (NSCLC). *J Clin Oncol* 37: 15s, 2019 (suppl; abstr:9036).

# Clinical Cancer Research

## HER3 Augmentation via Blockade of EGFR/AKT Signaling Enhances Anticancer Activity of HER3-Targeting Patritumab Deruxtecan in EGFR-Mutated Non–Small Cell Lung Cancer

Kimio Yonesaka, Junko Tanizaki, Osamu Maenishi, et al.

*Clin Cancer Res* 2022;28:390-403. Published OnlineFirst December 17, 2021.

<b>Updated version</b>	Access the most recent version of this article at: doi: <a href="https://doi.org/10.1158/1078-0432.CCR-21-3359">10.1158/1078-0432.CCR-21-3359</a>
<b>Supplementary Material</b>	Access the most recent supplemental material at: <a href="http://clincancerres.aacrjournals.org/content/suppl/2021/11/24/1078-0432.CCR-21-3359.DC1">http://clincancerres.aacrjournals.org/content/suppl/2021/11/24/1078-0432.CCR-21-3359.DC1</a>

<b>Cited articles</b>	This article cites 46 articles, 16 of which you can access for free at: <a href="http://clincancerres.aacrjournals.org/content/28/2/390.full#ref-list-1">http://clincancerres.aacrjournals.org/content/28/2/390.full#ref-list-1</a>
-----------------------	--

<b>E-mail alerts</b>	<a href="#">Sign up to receive free email-alerts</a> related to this article or journal.
----------------------	--

<b>Reprints and Subscriptions</b>	To order reprints of this article or to subscribe to the journal, contact the AACR Publications Department at <a href="mailto:pubs@aacr.org">pubs@aacr.org</a> .
-----------------------------------	--

<b>Permissions</b>	To request permission to re-use all or part of this article, use this link <a href="http://clincancerres.aacrjournals.org/content/28/2/390">http://clincancerres.aacrjournals.org/content/28/2/390</a> . Click on "Request Permissions" which will take you to the Copyright Clearance Center's (CCC) Rightslink site.
--------------------	--